Current Research in Food Science 6 (2023) 100419

Contents lists available at ScienceDirect

Current Research in Food Science

journal homepage: www.sciencedirect.com/journal/current-research-in-food-science

Encapsulation of vitexin-rhamnoside based on zein/pectin nanoparticles improved its stability and bioavailability

Xin Huang, Tuoping Li *, Suhong Li **

College of Food Science, Shenyang Agricultural University, Shenyang, 110866, China

ARTICLE INFO

Keywords:
Nanoencapsulation
Intestinal perfusion
In vitro digestion
Intestinal absorption

ABSTRACT

To improve the solubility, stability, and bioavailability of vitexin-rhamnoside (VR) isolated from hawthorn, it was encapsulated by the zein-pectin nanoparticles system. When the mass ratio of zein to pectin was 1:4, the particle size of nanoparticles was 222.7 nm, and the encapsulation efficiency of VR was 67%. Analysis with the scanning electron microscope (SEM), fourier transform infrared spectroscopy (FTIR) and atomic force microscopy (AFM) revealed that the zein-VR-pectin nanoparticles were spherical and uniformly distributed. The hydrogen bonding and electrostatic interactions were the main forces to assemble the nanoparticles. The nanoparticle had good stability at pH 3–8.5 with particle sizes ranging from 234 to 251 nm, and the nanoparticles were able to resist the relatively lower ionic strength. In vitro simulated digestion and rat in vivo intestinal perfusion experiments showed that the nanoparticles exhibited significant slow-release properties and the highest absorption rate in the duodenal segment of rats, with Ka and Papp of 0.830 ± 0.11 and 17.004 ± 1.09. These results provided a theoretical and technological approach for the construction of flavonoids delivery system with slow-release properties and improved bioavailability.

1. Introduction

Hawthorn (*Crataequs pinnatifida*), a famous rosaceous plant with beautiful flowers, is distributed worldwide and is cultivated and utilized as an important fruit in China for thousands of years. It also has been used as a food and medicinal homologous fruit in China, because of its multiple health benefit functionalities (Li et al., 2017). The major functional compounds in hawthorn are the flavonoids (Hou et al., 2020), and in which, vitexin-rhamnoside (VR) is the main bioactive component identified in our previous work (Huang et al., 2022) and the other research (Liang et al., 2007). VR has been proved to have multiple effects on treating hyperlipidemia, inhibiting α-glycosidase activity and increasing myocardial blood and oxygen supply, etc. (Zhu et al., 2006; Li et al., 2009). However, the stability of VR is lower which will restrict its processibility and absorbability in the body (Ying et al., 2007). It is also sensitive to changes in the external environment and is easily destroyed by gastric acid, resulting in low bioavailability and poor intestinal absorption due to its poor mucosal permeability (Lu et al., 2013).

Nanoencapsulation is widely regarded as a valuable method for improving the stability and functionality of bioactive substances (Fathi et al., 2018; Livney et al., 2003). Naturally occurring biomolecules, such as polysaccharides and proteins, are biocompatible, low immunogenic, non-toxic, and biodegradable, and therefore suitable for encapsulating bioactive substances (Assadpour, 2017). Preparation of nanoparticles of polysaccharides and proteins with hydrogen bonding and hydrophobic interactions to encapsulate bioactive substances can enhance their solubility and inhibit the oxidative breakdown in the gastrointestinal tract, sequentially increasing the absorption and bioavailability of such bioactive substances (Crini, 2019). Currently, a variety of techniques, such as solvent coprecipitation, pH-driven, solvent evaporation, and anti-solvent, have been established to assemble protein-polysaccharide complexes (Feng et al., 2020). The preparation of nanoparticles by anti-solvent is the most reported method, which is due to its simplicity and cost-effectiveness (Kaptay, 2012). The antisolvent method can be used for the preparation of nanoparticles not only of organic synthetic molecules but also mostly for the preparation of natural polyphenols (Ji et al., 2020).

Zein is generally perceived as a self-assembling material with non-sensitizing, adhesion, good film-forming characteristics, and biocompatibility (Luo and Wang, 2014). Changing the solvent polarity can

* Corresponding author. College of Food Science, Shenyang Agricultural University, Shenyang, 110086, China.
** Corresponding author. College of Food Science, Shenyang Agricultural University, Shenyang, 110086, China.
E-mail addresses: huangxin951220@163.com (X. Huang), litp@syau.edu.cn (T. Li), leesuhong@syau.edu.cn (S. Li).

https://doi.org/10.1016/j.crfs.2022.100419
Received 14 September 2022; Received in revised form 15 December 2022; Accepted 16 December 2022
Available online 18 December 2022

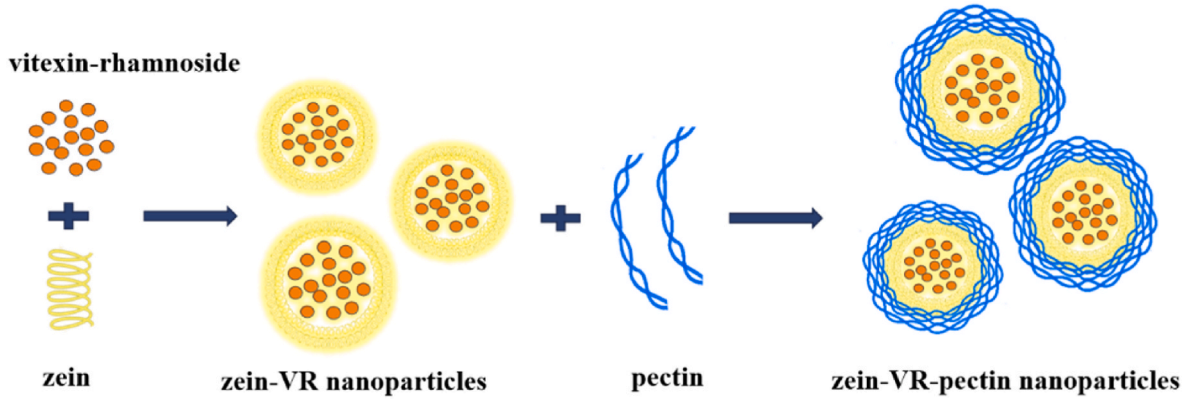

Fig. 1. The schematic diagram for the preparation of zein-VR-pectin nanoparticles.

induce the conformation change of the zein molecule, thus finally forming the nano-spherical particles. Based on these structural and functional properties, many zein-based nanoparticles have been successfully prepared (Chen et al., 2018; Sun et al., 2015). However, zein tends to be unstable and aggregation under high salt, high heat, or pH value near the isoelectric point (Patel et al., 2010). The main way to solve these problems is to add some stabilizers such as polysaccharides (Liu et al., 2020). Pectin, a complex polysaccharide widely existing in the plant cell wall, is a hydrophilic natural polymer with many functional properties. It is often used as a thickener, stabilizer, gelling agent, and the delivery carrier (Willats et al., 2006; Neufeld and Bianco-Peled, 2017). The pectin/zein core-shell nanoparticle has been constructed as a delivery carrier to improve the antioxidant activity of resveratrol (Huang et al., 2017). It has also been stated that the presence of pectin is beneficial to enhance the absorptivity of flavonoids in the body (Siemińska-Kuczer et al., 2022). On the other hand, pectin also can remain intact in the gastrointestinal environment and be utilized by microorganisms in the colon (Teixe-Roig et al., 2020). Based on these advantages, the objective of the current research was to construct a zein-VR-pectin nanoparticle delivery system for loading and improving the stability and in vivo bioavailability of VR.

2. Materials and methods

2.1. Materials

Hawthorn fruit (*Crataegus pinnatifida,* variety of *Mengyin dajinxing*) was collected from the National Germplasm Resources Garden of Hawthorn located at Shenyang Agricultural University. After removing the core, the hawthorn was freeze-dried and ground as powder with a high-speed grinder and sieved through 40 mesh. Hawthorn flavonoids were extracted from hawthorn powder with 60% ethanol at 50 °C.

Vitexin-rhamnoside was isolated and purified by HP-20 macroporous resin (column, 2 × 20 cm; eluent, 70% ethanol) and semi-preparative liquid chromatography (LC-3000 liquid chromatography system (Shimadzu, Japan) equipped with a SHIMADZU ODS column (20 × 250 mm); mobile phases were 0.1% formic acid in water (A) and 0.1% formic acid in acetonitrile (B); the elution program was 0–55 min of 95%–0% phase A and 55–60 min of 100% phase B. The purity of VR was more than 95% measured by high-pressure liquid chromatography (Waters H-Class High-Performance Liquid Chromatograph (Waters, USA); a Thermo AQUASIL C18 column (4.6 × 250 mm) was used with the solvent of 0.1% formic acid in water and 0.1% formic acid; the elution program was same as the condition of semi-preparative liquid chromatography mentioned above).

Zein was purchased from Yifa Biotech Co., Ltd. Apple, citrus, and sunflower pectin were obtained from Fuyuan pectin Co., Ltd. Other chemical reagents used were of analytical grade.

2.2. Preparation of zein-VR-pectin nanoparticles

Zein-VR-pectin nanoparticles were prepared by the anti-solvent precipitation method. Zein and vitexin-rhamnoside were dissolved in ethanol and stirred at 600 rpm for 2h. The apple, citrus, and sunflower pectin was dissolved in hot water and stirred for 2h, respectively (The mass ratio of different pectin and zein was 1:1). The ethanol solution of zein and vitexin-rhamnoside was poured into the pectin solution in a uniform trickle and stirred at 600 rpm for 5h. After that, ethanol was removed by rotary evaporation (60 °C) and supplemented to the original volume with distilled water to obtain nanoparticles. The schematic diagram of the preparation of zein-VR-pectin nanoparticles was shown in Fig. 1.

2.3. Nanoparticle characterization

2.3.1. Zeta potential measurements and particle size

Zeta potential (mV), particle size (nm), and PDI were measured by the Zetasizer nano potentiometer (NanoZS90, Malvern Instruments Ltd.) at 25 °C (Liu et al., 2021).

2.3.2. Encapsulation efficiency

Exactly 1 mL of the freshly prepared nanoparticles dispersion was mixed with 5 mL anhydrous ethanol, followed by ultrasonication for 10 min to extract VR, then centrifuged at 4000 rpm for 10 min, the precipitates were extracted again in the same way. The supernatant was collected and combined. The VR content was detected by a UV spectrophotometer (Beijing, China) at 334 nm, and calculated by the following equation: $Y = 0.057X + 0.0268$ ($R^2 = 0.9992$), where X was the concentration of VR (μg/mL), Y was the absorbance at corresponding wavelengths. The encapsulation efficiency was calculated as equation (1)(Niu et al., 2021):

$$\text{Encapsulation efficiency}(\%) = \frac{\text{mass of VR in nanoparticles}}{\text{total mass of VR used}} \quad (1)$$

2.4. Scanning electron microscopy (SEM)

The morphology of nanoparticles was analyzed by scanning electron microscopy (Tianmei, China). The freeze-dried nanoparticles were fixed on the double-sided tape installed on the aluminum column, coated with the platinum film under vacuum, and placed in the SEM 10 kV accelerating voltage low vacuum mode to observe the amplified sample structure (Torres et al., 2017).

2.5. Atomic force microscopy (AFM)

AFM images of Zein-VR-pectin nanoparticles were taken using a Hitachi AFM-5500M atomic force microscope (Hitachi Ltd., Tokyo,

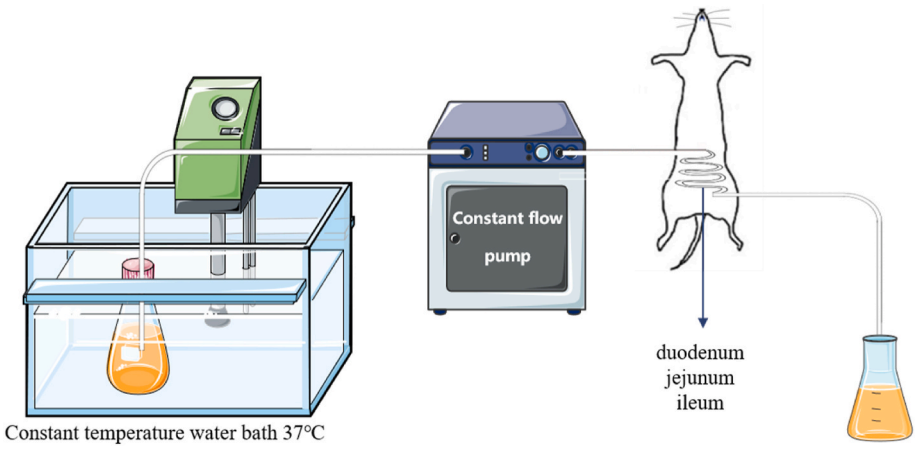

Fig. 2. In vivo intestinal perfusion model of rats.

Japan) equipped with a fully addressable 4-inch stage, which eliminated the requirement for sample remount. The Zein-VR-pectin nanoparticles were dissolved in deionized water to prepare an aqueous solution of 5 mg/mL 10 μl solution was dropped onto the clean mica plate and dried naturally. Tap-mode was selected for AFM imaging analysis (NX20, Bruker Co., USA) (Zhao et al., 2020).

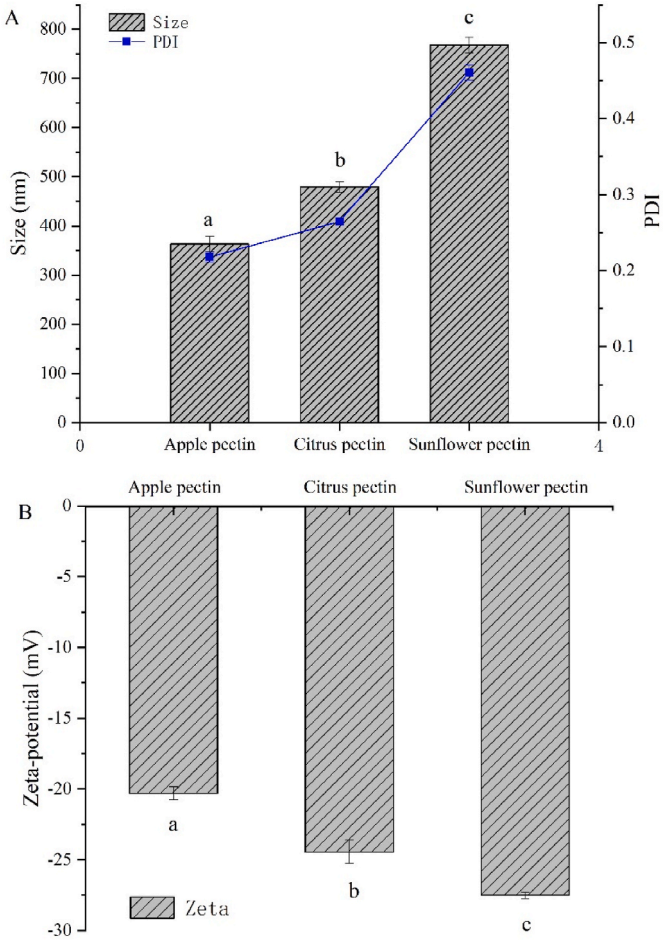

Fig. 3. Effect of the different pectin (apple, citrus, sunflower) on the size, PDI (A), and zeta-potential (B) of the composite nanoparticles. Different letters indicate significant differences between samples ($p < 0.05$).

2.6. Fourier transform infrared spectroscopy (FTIR)

Samples were loaded on the dried KBr and subjected to Fourier transform infrared spectra (Tianjin Tuopu Instrument Co., China) with a scan wave range of 4000-400 cm^{-1} and a resolution of 2 cm^{-1} (Rampino et al., 2016).

2.7. Stability analysis

2.7.1. pH stability

The freshly prepared colloidal suspension was mixed with 10 mM citric acid phosphate buffer (pH 3.0–8.5). If necessary, the pH of the mixture was adjusted by 1 mol/L NaOH or HCl. The change in particle size of nanoparticles was detected.

2.7.2. Salt ion stability

Zein-VR-pectin nanoparticles were added into a 0–0.6 mol/L NaCl, KCl, $MgCl_2$, and $CaCl_2$ solutions, respectively, and stood at room temperature for 24 h. The average particle size, PDI, and zeta potential of the samples were measured.

2.8. In vitro digestion of zein-VR-pectin nanoparticles

0.1g nanoparticles were dissolved in 20 ml distilled water and stirred for 1h. The nanoparticles dispersions were then mixed with 20 mL of simulated gastric fluid (double distilled water adjusted to pH 2.0 with HCl, containing 50 mM NaCl, and 7000U/mL pepsin). The mixtures were adjusted to pH 2.0 and digested at 37 °C for 2h. After gastric digestion, digestive juices were adjusted to pH 7.0 with 1.0 M NaOH. The gastric digestive juice was then added to simulated intestinal fluid and digested at 37 °C for 4h with the pH values of the digestion stage at 7.0. The release of vitexin-rhamnoside was measured every 1h (Zhao et al., 2020).

2.9. In vivo intestinal perfusion experiment in rats

The animal experiments were conducted following a guideline approved by the Experimental Animal Commission of Shenyang Agricultural University, the IACUC number protocol is 2022030702. This protocol conforms with the "Guiding Principles in the Care and Use of Animals (China)" for the care and use of laboratory animals. Four-week-old SD female rats (Beijing Huafukang Biotechnology Co., Ltd.) with a body weight of 200 ± 20 g were ready for use after quarantine. After a week of acclimatization, the rats were fasted for 18 h (free drinking water) and anesthetized by intraperitoneal injection of urethane solution (1 g/kg) with the appropriate dose, to ensure that the duration of deep anesthesia was enough for excremental operation. After the rat

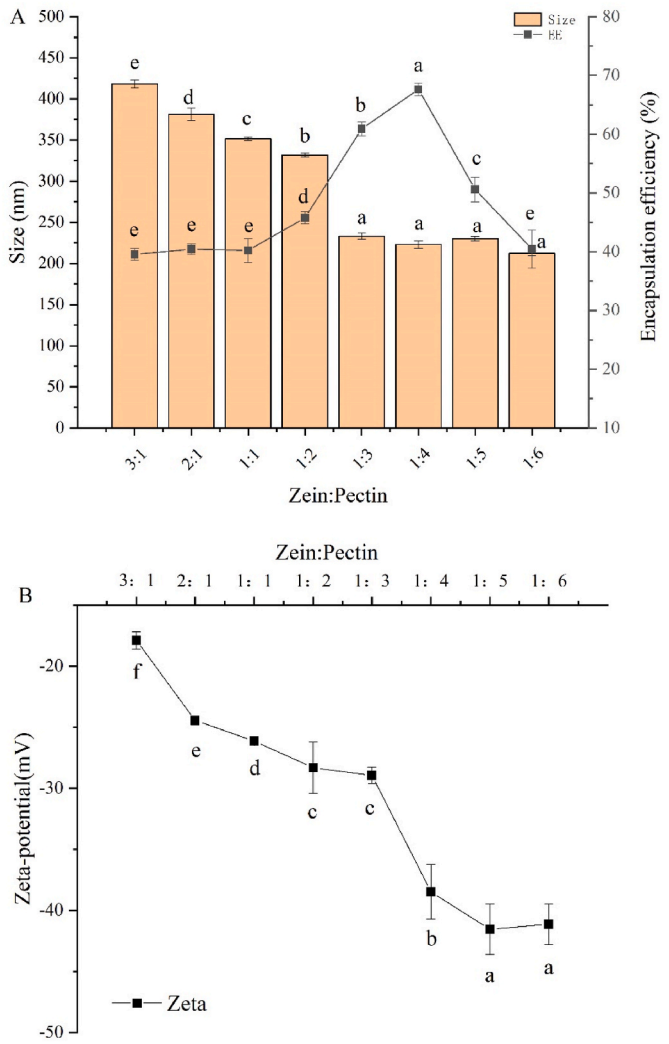

Fig. 4. Effect of the zein to pectin mass ratio on the size and encapsulation efficiency (EE) (A) and Zeta-potential (B) of zein-VR-pectin nanoparticles. Different letters indicate significant differences between samples ($p < 0.05$).

went into deep anesthesia, the abdominal cavity was opened, and intestinal perfusion experiments were performed on the duodenum, jejunum, and ileum, respectively, with 10 cm of each section of the intestine (Fig. 2). The plastic tubing was set at both ends of the small intestine to connect the intestine and sample solution. The intestinal contents were washed with normal saline and then perfused in the sample solution at 0.3 ml/min for 2h. The constant temperature of the entire process was 37 °C. During the experiment, the rats were monitored in real-time whether they maintain a deep anesthesia state by the skin pinch reaction, corneal reflex, and respiratory rate. In case there were signs of pain and awakening, urethane solution will be immediately supplemented to keep the deep-anesthesia. At the end of the experiment, the rats were euthanized with an overdose of anesthetic. The weight method was used to correct the volume of circulating fluid in this experiment. The residual content of VR was measured, and the absorption rate constant (Ka), apparent permeability coefficient (Papp), and cumulative absorption (A) of vitexin-rhamnoside were calculated as equations (2) and (3) (Ying et al., 2007).

$$K_a = \left(1 - \frac{C_{out}}{C_{in}} \times \frac{V_{out}}{V_{in}}\right) \times \frac{Q_{in}}{\pi r^2 L} \quad (2)$$

$$Papp = \frac{-Q_{in} \ln \frac{C_{out}}{C_{in}} \times \frac{V_{out}}{V_{in}}}{2\pi r L} \quad (3)$$

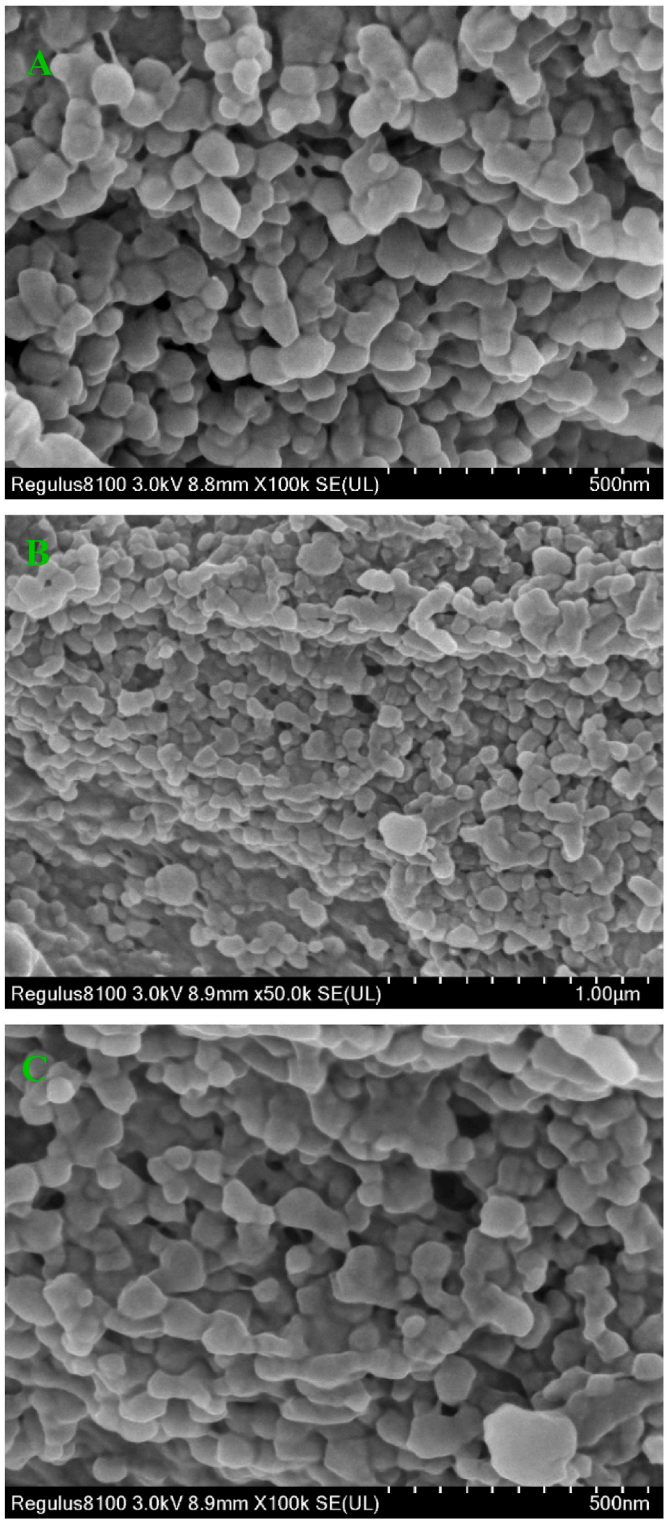

Fig. 5. SEM images of the Zein-Pectin nanocarriers with a magnification of 100k (A), and Zein-VR-Pectin nanocarriers with a magnification of 50k (B), 100k (C).

2.10. Statistical analysis

All experiments were repeated at least three times. The data were analyzed by ANOVA with SPSS 26.0 software (SPSS Inc., Chicago, IL, USA). $P < 0.05$ was regarded as statistically significant and $p < 0.01$ as very significant.

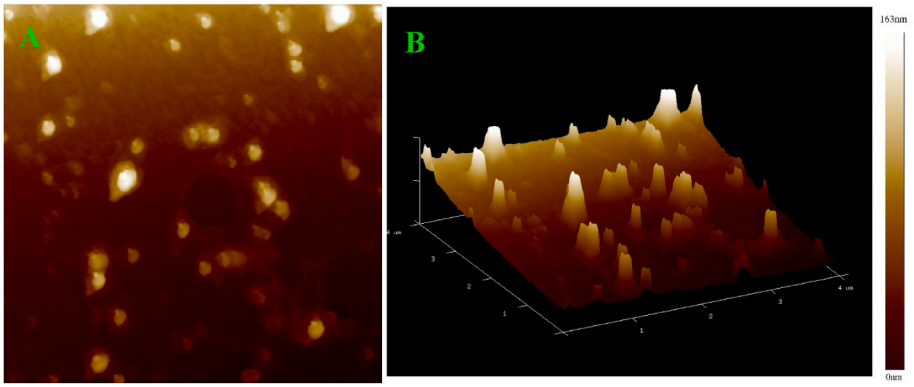

Fig. 6. AFM images of zein-VR-pectin nanoparticles in a two-dimensional plane (A) and three-dimensional morphology (B).

3. Results and discussion

3.1. Effect of the pectin to zein mass ratio on the mean size, PdI, and zeta-potential of zein-VR-pectin nanoparticles

The behaviors of different pectin on the composite nanoparticles were investigated (Fig. 3). The nanoparticles prepared with apple pectin were smaller in size and PDI, and the nanoparticles were more uniformly distributed, compared with those prepared with citrus pectin and sunflower pectin. Therefore, apple pectin was chosen for the subsequent experiments.

The effect of different mass ratios of zein/pectin on the size and encapsulation efficiency were shown in Fig. 4A. The particle size gradually decreased but the encapsulation efficiency gradually increased with the ratio of zein and pectin varied from 3:1 to 1:3, then tend to be stable, indicating that the size of nanoparticles was depended on the pectin concentration. A small amount of pectin on the surface of zein was not enough to resist the aggregation of zein, resulting in relatively larger particle size of zein-VR-pectin nanoparticles (Hu and McClements, 2015). With the increase of pectin concentration, the surface negative charge of nanoparticles gradually increased, and the electrostatic repulsion was enhanced to inhibit the aggregation of particles (Dai et al., 2018).

Meanwhile, the ζ-potential of nanoparticles was also decreased with the increase in the mass ratio of pectin/zein (Fig. 4B). With the increased of pectin, more pectin molecules were adsorbed to the surface of nanoparticles, which maked its negative ζ-potential increased, and the stability of the particles increased due to classical repulsion until the pectin adsorption on the particle surface reaches saturation (1:5) when the potential of the particles no longer decreased and formed a stable dispersion (Peinado et al., 2010).

In addition, the maximum encapsulation efficiency of VR was found at a mass ratio of 1:4. Together with the above results, the zein/pectin of 1:4 was considered a suitable ratio to prepare the zein-VR-pectin nanoparticles with the encapsulation efficiency of 67.6%.

3.2. SEM and AFM characterization of zein-VR-pectin nanoparticles

The SEM of zein-VR-pectin nanoparticles were shown in Fig. 5A and B. The composite nanoparticles were spherical in shape, uniform in size, and tightly bound. Most of the particles ranged from 100 to 200 nm, and there were also a few particles with smaller particle size. This was due to the particles existed in the dry state by SEM, so the particle size measured by the laser particle sizer was slightly larger than that by SEM. When the particles existed in the solution, the surface was covered by a hydration layer. In the process of natural drying, the surface water volatilized into the air, the nanoparticles would have obvious water loss shrinkage (Wang et al., 2013; Zhu et al., 2013). Compared with Zein-pectin blank particles (Fig. 5C), the addition of VR seemed did not cause changes in particle morphology. This phenomenon was similar to zein-resveratrol -chitosan in that the loading of resveratrol also would not alter the morphology of zein-chitosan nanoparticles (Khan et al., 2021).

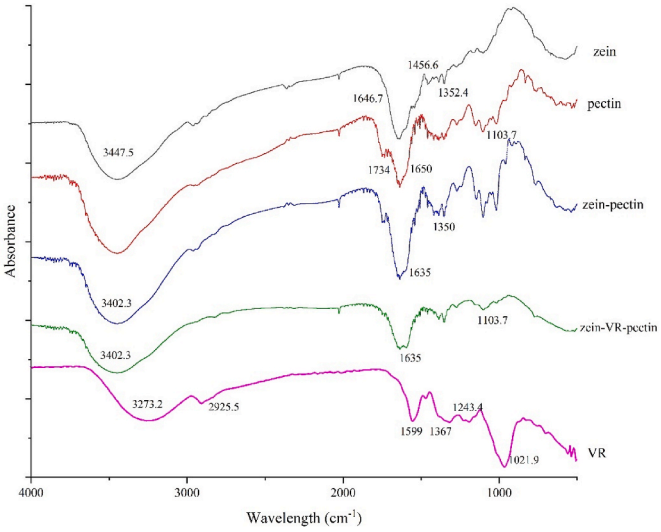

Fig. 7. FTIR of VR, zein, pectin, Zein-Pectin, and Zein-VR-Pectin.

From the AFM (Fig. 6) images, the zein-VR-pectin nanoparticles showed a monodisperse distribution. The aggregation height of the nanocarriers was 163 nm. The micelle size observed at this time was smaller than that of the micrometer because of protein dehydration during AFM sample preparation. This was consistent with the SEM results.

3.3. FT-IR spectrometry

According to the FT-IR spectrum in Fig. 7, VR had infrared absorption peaks at 3273.2, 1599, and 1021.9 cm^{-1}, which are due to the C–H bond stretching, C–C stretching, and C–O bond stretching vibration, respectively (Patle et al., 2020). And VR sample has a weak absorption peak at 2925.5 cm-1, which is an antisymmetric stretching vibration peak of the methylene C–H bond. zein exhibited obvious infrared absorption peaks at 3447.53, 1646.7, 1456.65, and 1352.40 cm^{-1}, which are attributed to the N–H bond vibration stretching, C–O stretching (amide I), NH_2 in-plane deformation vibration (amide II) and C–N bond stretching vibration (amide III), respectively (Hu et al., 2015). Peaks at 1650 cm^{-1} and 1734 cm^{-1} were the characteristic free and esterified carboxyl groups of pectin, respectively (Yan et al., 2017). The peaks between 1100 and 1200 cm^{-1} were assigned to the C–O–C and C–C

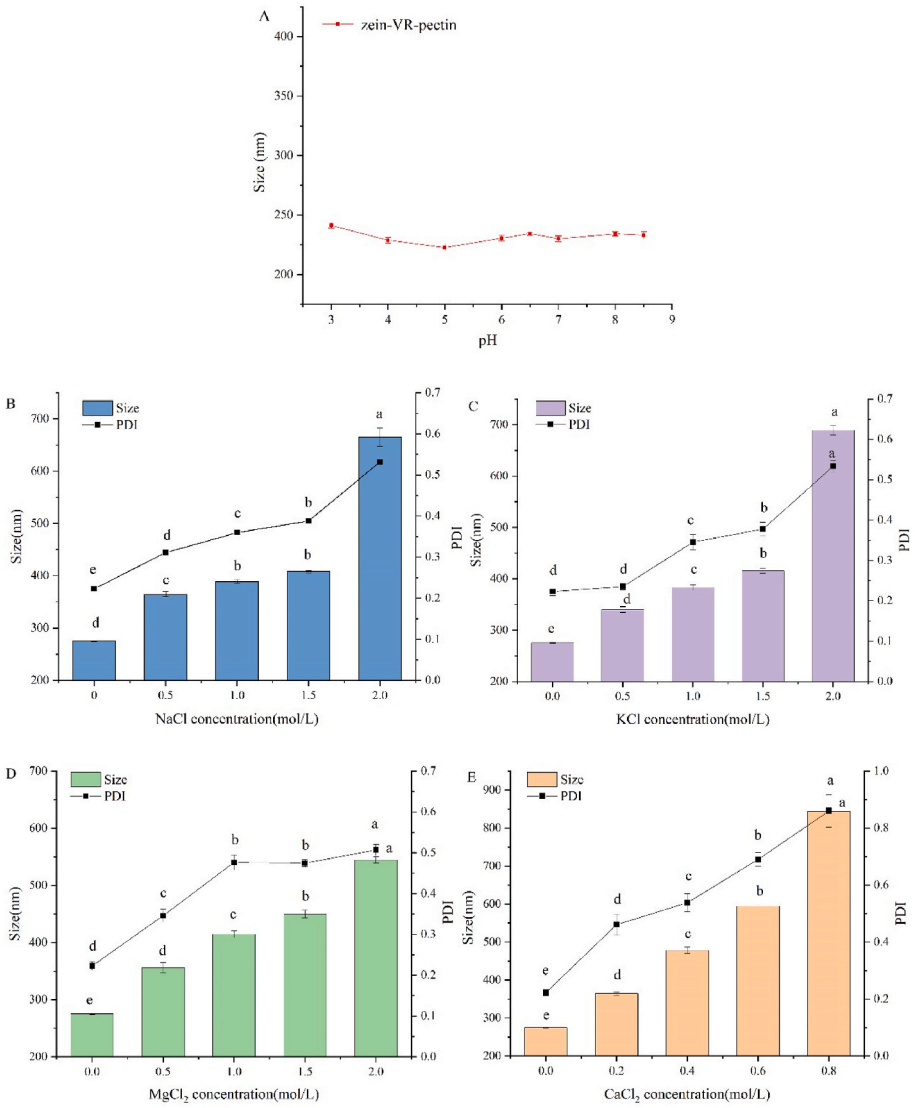

Fig. 8. Effect of the pH value on the size of zein-VR-pectin nanoparticles(A), and effect of salt ion stability (B. NaCl, C. KCl, D. $MgCl_2$, E. $CaCl_2$) on size and PDI of zein-VR-pectin nanoparticles. Different letters indicate significant differences between samples ($p < 0.05$).

bonds of pectin. Compared with zein, the nanoparticles of zein-pectin shifted the N–H bond peak from 3447.53 to 3402.3 cm^{-1}, indicating that there was a hydrogen bond interaction formed between zein and pectin (Sun et al., 2017). The peaks of C–O stretching (amide I) and C–N stretching vibration were also shifted to 1635.75 and 1350.4 cm^{-1}, respectively. That might be caused by the electrostatic interactions between zein and pectin (Wang et al., 2020).

After loading of VR to the zein-pectin nanoparticles, the intensity of peaks at 1386.5 and 1350.4 cm^{-1} was significantly decreased, which might be due to the spatial conformation changes caused by molecule interactions of VR and zein with the hydrogen bond and hydrophobic interaction, resulting in the reduced or disappeared infrared absorption intensity (Livesay et al., 2008). Meanwhile, the characteristic peaks of VR at 1021.9 and 1243.4 completely disappeared, which proved that VR was completely embedded in nanoparticles. These results also suggested that there were not only hydrogen bonds but also electrostatic and hydrophobic interactions that functioned in the formation of zein-VR-pectin nanoparticles.

3.4. Effect of pH and salt ions on the stability of nanoparticles

The variation of zein-VR-pectin nanoparticle size with pH were shown in Fig. 8A. The zein-VR-pectin nanoparticle showed the excellent stability against aggregation at pH 3–8.5 with particle sizes ranging from 234 to 251 nm. Minimum particle size of 222 nm was obtained at pH 5. The particle size was almost the same as that of the original dispersion, showing no sign of particle destabilization.

The effect of salt ions on the stability of zein-VR-pectin nanoparticles were shown in Fig. 8B–E. The particle size and PDI of nanoparticles were concentration-dependently increased with the increase of salt ion concentrations. Whether monovalent ions or divalent ions, the increase slops were much higher at higher ion concentrations (0.8 mol/L for Ca^{2+}, and 2.0 mol/L for Na^{+}, K^{+}, and Mg^{2+} ions) than those at lower concentrations, indicating that zein-VR-pectin nanoparticles was able to resist to the relatively lower ionic strength. Additionally, zein-VR-pectin nanoparticles seemed to be more sensitive to Ca^{2+} ions than other ions used here.

3.5. In vitro gastrointestinal digestion of zein-VR-pectin nanoparticles

Effective protection and sustained release of bioactive compounds in the gastrointestinal digestive system are essential for the evaluation of food carriers (Hou et al., 2014). The in vitro gastrointestinal digestion of Zein-VR-Pectin nanoparticles was shown in Fig. 9. In the gastric juice,

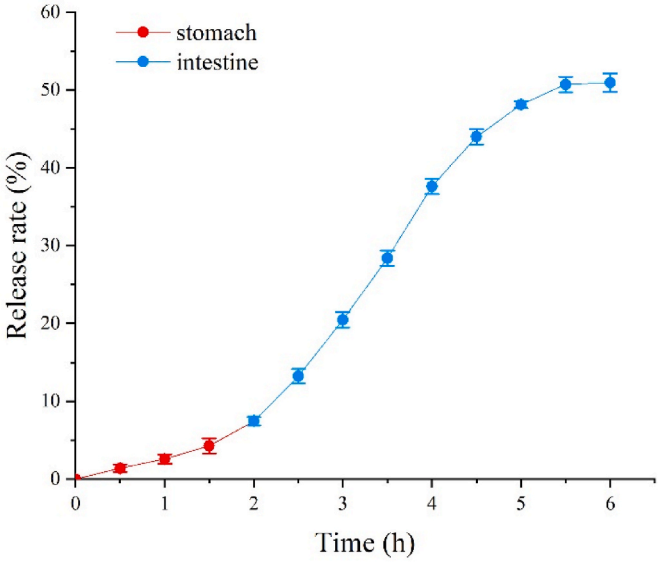

Fig. 9. In vitro digestion of zein-VR-pectin nanoparticles.

Table 1
Absorption parameters of zein-VR-pectin nanoparticles and VR in rat intestines in situ.

Intestinal segment	zein-VR-pectin nanoparticles		Free-VR	
	K_a ($\times 10^{-1}$ min•$^{-1}$)	Papp ($\times 10^{-3}$ cm min^{-1})	K_a ($\times 10^{-1}$ min•$^{-1}$)	Papp ($\times 10^{-3}$ cm min^{-1})
Duodenum	0.830 ± 0.11a	17.004 ± 1.09a	0.217 ± 0.03a	3.476 ± 0.14a
Jejunum	0.580 ± 0.05b	10.717 ± 0.78b	0.134 ± 0.05b	2.092 ± 0.22b
Ileum	0.336 ± 0.04c	5.59 ± 0.08c	0.106 ± 0.02b	1.640 ± 0.11c

Different superscript letters in the same column indicate significant differences ($p < 0.05$).

the release rate of VR in the nanoparticles was 7.4%. However, it in the intestinal fluid raised to 51%, significantly higher than that in simulated gastric fluids.

The free VR is unstable and its bioavailability also is very low in the body, since it is very easily destroyed by gastric acid, thus difficult to enter the small intestine to be absorbed and utilized (Lu et al., 2013). After being encapsulated in the core-shell structure of zein-pectin nanoparticles, the VR effectively resisted the destruction of gastric acid and pepsin that 92.6% VR was retained in the zein-pectin nanoparticles, and could be allowed to flow into the small intestine for use. The small intestine is an important organ for the absorption of nutrients and functional substances. When the zein-VR-pectin nanoparticles passed into the intestine, the altered pH environment enabled it to alter its "shell" structure to slowly release the target component VR from zein-VR-pectin nanoparticles in the intestine (Li and Yu, 2020), such structural changes and sustained release properties were expectant and beneficial for absorption and utilization of VR in the body. Such core-shell encapsulation systems were also well used to improve the in vivo absorption rate and bioavailability of functional substances. For example, quercetin was subjected to the zein-Que-HA encapsulation system to improve its intestinal absorption rate, and this nanoparticle system with the sustained release properties has enhanced the absorption and bioavailability of Quercetin (Chen et al., 2019).

3.6. Intestinal absorption of zein-VR-pectin nanoparticles in situ of rats

It is generally accepted that the in vivo absorption experiment can ensure the activities of digestive enzymes in the intestinal contents (Dahlgren et al., 2020). The absorption capacity of a substance in the intestine is mainly evaluated by the intestinal wall permeability of the substance, such as the absorption rate constant (Ka) and the apparent permeability coefficient (Papp). Generally, substances in the intestine are difficult to be absorbed when Papp $<3 \times 10\text{-}6$ cm/s, whereas are easy to absorb at Papp $> 2 \times 10\text{-}5$ cm/s (Fagerholm et al., 1996).

Based on the good results obtained from in vitro simulated digestion experiments mentioned above, the in vivo intestinal perfusion method was further used to explore the absorption behaviors of VR from zein-VR-pectin nanoparticles in the intestine. Table 1 showed that both Papp and Ka of VR in zein-VR-pectin nanoparticles were markedly higher than those of free-VR in the duodenum, jejunum, and ileum, indicating that VR of nanoparticles was well absorbed in each intestinal segment of the small intestine, and the bioavailability of VR in the zein-VR-pectin nano-system was superior to that of the free form of VR in the small intestine.

The protein-polysaccharide system is well used to enhance the stability and intestinal absorption of target substances (Xu et al., 2020), since the nano-sized particle more easily passes through the exclusion layer of the intestine and is more readily absorbed by the epithelial cells of the small intestine compared to the raw material, to improve the bioavailability of nutrients in the matrix (Porter et al., 2007). Meanwhile, the polysaccharide-protein nanoparticles have better mucosal adhesion ability to adhere to epithelial cells, increase the residence time of the loaded compounds, and provide sustained release and targeted delivery of the compounds at the site of intestinal absorption (Ensign et al., 2012). Li et al. (2022) have reported that peptide (CSKSSDYQC)-vitexin-chitosan (TMC) nanoparticles have improved the intestinal absorption and bioavailability of vitexin. The caseinate-quercetin-zein nanoparticles prepared by Zhou et al. (2021) have increased the passive diffusion rate of quercetin and thereby increased its bioavailability. On the other hand, it has been confirmed that the coexistence of pectin and flavonoids can improve the absorption efficiency and bioavailability of flavonoids (Tomas et al., 2020; Jakobek and Matić, 2019). Our present results that zein-VR-pectin nanoparticles improved the absorption and utilization efficiencies of VR in vivo might be also partially related to that mechanism. However, the underlying roles and mechanisms require further investigations.

4. Conclusion

Zein-VR-pectin nanoparticles have been successfully prepared using an anti-solvent method. The pectin and protein formed a composite nanoparticle by electrostatic interactions, and the hawthorn flavonoids were bound to zein by hydrophobic interaction and hydrogen bonds. The pectin and protein formed a composite nanoparticle by electrostatic interactions, and the hawthorn flavonoids were bound to zein by hydrophobic interaction and hydrogen bonds. The release and absorption of the nanoparticles were also investigated in vitro and in vivo, and it was demonstrated that the nanoparticles have good slow release, and the release rate in the small intestine can reach 51%. Zein-VR-pectin nanoparticles significantly improved the bioavailability of VR, the particles were best absorbed in the duodenum of rats. This study provided a basis for promoting the oral stability and absorptivity of VR. The results are also valuable for the flavonoids related bioactive-compounds to ameliorate their bioavailability, thus increasing their contribution to healthy living.

CRediT authorship contribution statement

Xin Huang: Data curation, Formal analysis, Methodology, Software, Writing – original draft, Writing – review & editing. **Tuoping Li:** Conceptualization, Project administration, Supervision, Validation, Writing – review & editing. **Suhong Li:** Conceptualization, Project administration, Supervision.

Declaration of competing interest

The authors declare that they have no known competing financial interests or personal relationships that could have appeared to influence the work reported in this paper.

Data availability

The data that has been used is confidential.

References

Assadpour, E., 2017. Protection of phenolic compounds within nanocarriers, CAB reviews: perspectives in agriculture, veterinary science. Nutr. Nat. Resources 12. https://doi.org/10.1079/PAVSNNR201712057.

Chen, S., Sun, C.X., Wang, Y.Q., Han, Y.H., Dai, L., Abliz, A., Gao, Y.X., 2018. Quercetagetin-loaded composite nanoparticles based on zein and hyaluronic acid: formation, characterization, and physicochemical stability. J. Agric. Food Chem. 66 (28), 7441–7450. https://doi.org/10.1021/acs.jafc.8b01046.

Chen, S., Han, Y., Wang, Y., Yang, X., Sun, C., Mao, L., Gao, Y., 2019. Zein-hyaluronic acid binary complex as a delivery vehicle of quercetagetin: fabrication, structural characterization, physicochemical stability and in vitro release property. Food Chem. 276, 322–332. https://doi.org/10.1016/j.foodchem.2018.10.034.

Crini, G., 2019. Historical review on chitin and chitosan biopolymers. Environ. Chem. Lett. 17 (4), 1623–1643. https://doi.org/10.1007/s10311-019-00901-0.

Dahlgren, D., Sjogren, E., Lennernas, H., 2020. Intestinal absorption of BCS class II drugs administered as nanoparticles: a review based on in vivo data from intestinal perfusion models. Admet & Dmpk 8 (4), 375–390. https://doi.org/10.5599/admet.881.

Dai, L., Li, R., Wei, Y., Sun, C., Mao, L., Gao, Y., 2018. Fabrication of zein and rhamnolipid complex nanoparticles to enhance the stability and in vitro release of curcumin. Food Hydrocolloids 77, 617–628. https://doi.org/10.1016/j.foodhyd.2017.11.003.

Ensign, L.M., Cone, R., Hanes, J., 2012. Oral drug delivery with polymeric nanoparticles: the gastrointestinal mucus barriers. Adv. Drug Deliv. Rev. 64 (6), 557–570. https://doi.org/10.1016/j.addr.2011.12.009.

Fagerholm, U., Johansson, M., Lennernäs, H., 1996. Comparison between permeability coefficients in rat and human jejunum. Pharm. Res. (N. Y.) 13 (9), 1336–1342. https://doi.org/10.1023/A:1016065715308.

Fathi, M., Donsi, F., McClements, D.J., 2018. Protein-based delivery systems for the nanoencapsulation of food ingredients. Compr. Rev. Food Sci. Food Saf. 17 (4), 920–936. https://doi.org/10.1111/1541-4337.12360.

Feng, S., Sun, Y., Wang, D., Sun, P., Shao, P., 2020. Effect of adjusting pH and chondroitin sulfate on the formation of curcumin-zein nanoparticles: synthesis, characterization and morphology. Carbohydr. Polym. 250, 116970 https://doi.org/10.1016/j.carbpol.2020.116970.

Hou, Z., Liu, Y., Lei, F., Gao, Y., 2014. Investigation into the in vitro release properties of β-carotene in emulsions stabilized by different emulsifiers. LWT - Food Sci. Technol. (Lebensmittel-Wissenschaft -Technol.) 59 (2, Part 1), 867–873. https://doi.org/10.1016/j.lwt.2014.07.045.

Hou, W.Z., Wang, Y.T., Wang, W., Zhi, M.L., Gou, X.L., Qian, C., Zhang, F., 2020. Determination and evaluation of flavonoids in hawthorn in China. J. Biobased Mater. Bioenergy 14 (5), 664–669. https://doi.org/10.1166/jbmb.2020.2003.

Hu, K., McClements, D.J., 2015. Fabrication of biopolymer nanoparticles by antisolvent precipitation and electrostatic deposition: zein-alginate core/shell nanoparticles. Food Hydrocolloids 44, 101–108. https://doi.org/10.1016/j.foodhyd.2014.09.015.

Hu, K., Huang, X., Gao, Y., Huang, X., Xiao, H., McClements, D.J., 2015. Core–shell biopolymer nanoparticle delivery systems: synthesis and characterization of curcumin fortified zein–pectin nanoparticles. Food Chem. 182, 275–281. https://doi.org/10.1016/j.foodchem.2015.03.009.

Huang, X.L., Dai, Y.Q., Cai, J.X., Zhong, N.J., Xiao, H., McClements, D.J., Hu, K., 2017. Resveratrol encapsulation in core-shell biopolymer nanoparticles: impact on antioxidant and anticancer activities. Food Hydrocolloids 64, 157–165. https://doi.org/10.1016/j.foodhyd.2016.10.029.

Huang, X., Bian, Y., Liu, T., Xu, Z., Song, Z., Wang, F., Li, T., Li, S., 2022. Antioxidant potential and in vitro inhibition of starch digestion of flavonoids from Crataegus pinnatifida. Heliyon 8 (10), e11058. https://doi.org/10.1016/j.heliyon.2022.e11058.

Jakobek, L., Matić, P., 2019. Non-covalent dietary fiber - polyphenol interactions and their influence on polyphenol bioaccessibility. Trends Food Sci. Technol. 83, 235–247. https://doi.org/10.1016/j.tifs.2018.11.024.

Ji, S., Jia, C., Cao, D., Muhoza, B., Zhang, X., 2020. Formation, characterization and properties of resveratrol-dietary fiber composites: release behavior, bioaccessibility and long-term storage stability. LWT 129, 109556. https://doi.org/10.1016/j.lwt.2020.109556.

Kaptay, G., 2012. On the size and shape dependence of the solubility of nano-particles in solutions. Int. J. Pharm. 430 (1), 253–257. https://doi.org/10.1016/j.ijpharm.2012.03.038.

Khan, M.A., Chen, L., Liang, L., 2021. Improvement in storage stability and resveratrol retention by fabrication of hollow zein-chitosan composite particles. Food Hydrocolloids 113, 106477. https://doi.org/10.1016/j.foodhyd.2020.106477.

Li, M., Yu, M., 2020. Development of a nanoparticle delivery system based on zein/polysaccharide complexes. J. Food Sci. 85 (12), 4108–4117. https://doi.org/10.1111/1750-3841.15535.

Li, H., Song, F., Xing, J., Tsao, R., Liu, Z., Liu, S., 2009. Screening and structural characterization of α-glucosidase inhibitors from hawthorn leaf flavonoids extract by ultrafiltration LC-DAD-MSnand SORI-CID FTICR MS. J. Am. Soc. Mass Spectrom. 20 (8), 1496–1503. https://doi.org/10.1016/j.jasms.2009.04.003.

Li, S., Huang, Z., Dong, Y., Zhu, R., Li, T., 2017. Haw pectin pentaglaracturonide inhibits fatty acid synthesis and improves insulin sensitivity in high-fat-fed mice. J. Funct. Foods 34, 440–446. https://doi.org/10.1016/j.jff.2017.04.030.

Li, S., Lv, H., Chen, Y., Song, H., Zhang, Y., Wang, S., Luo, L., Guan, X., 2022. N-trimethyl chitosan coated targeting nanoparticles improve the oral bioavailability and antioxidant activity of vitexin. Carbohydr. Polym. 286, 119273 https://doi.org/10.1016/j.carbpol.2022.119273.

Liang, M., Xu, W., Zhang, W., Zhang, C., Liu, R., Shen, Y., Li, H., Wang, X., Wang, X., Pan, Q., Chen, C., 2007. Quantitative LC/MS/MS method and in vivo pharmacokinetic studies of vitexin rhamnoside, a bioactive constituent on cardiovascular system from hawthorn. Biomed. Chromatogr. 21 (4), 422–429. https://doi.org/10.1002/bmc.777.

Liu, Q.Y., Chen, J.J., Qin, Y., Jiang, B., Zhang, T., 2020. Zein/fucoidan-based composite nanoparticles for the encapsulation of pterostilbene: preparation, characterization, physicochemical stability, and formation mechanism. Int. J. Biol. Macromol. 158, 461–470. https://doi.org/10.1016/j.ijbiomac.2020.04.128.

Liu, K., Zha, X.-Q., Li, Q.-M., Pan, L.-H., Luo, J.-P., 2021. Hydrophobic interaction and hydrogen bonding driving the self-assembling of quinoa protein and flavonoids. Food Hydrocolloids 118, 106807. https://doi.org/10.1016/j.foodhyd.2021.106807.

Livesay, D.R., Huynh, D.H., Dallakyan, S., Jacobs, D.J., 2008. Hydrogen bond networks determine emergent mechanical and thermodynamic properties across a protein family. Chem. Cent. J. 2, 17. https://doi.org/10.1186/1752-153x-2-17, 17.

Livney, Y.D., Corredig, M., Dalgleish, D.G., 2003. Influence of thermal processing on the properties of dairy colloids. Curr. Opin. Colloid Interface Sci. 8 (4), 359–364. https://doi.org/10.1016/S1359-0294(03)00092-X.

Lu, D., Zhang, W.j., Zou, H.j., Xue, H., Yin, J., Chen, Y., Ying, X., Kang, T., 2013. Bioavailability of vitexin-2"-O-rhamnoside after oral Co-administration with ketoconazole, verapamil and bile salts. Lat. Am. J. Pharm. 32 (8), 1218–1223.

Luo, Y., Wang, Q., 2014. Zein-based micro- and nano-particles for drug and nutrient delivery: a review. J. Appl. Polym. Sci. 131 (16) https://doi.org/10.1002/app.40696.

Neufeld, L., Bianco-Peled, H., 2017. Pectin-chitosan physical hydrogels as potential drug delivery vehicles. Int. J. Biol. Macromol. 101, 852–861. https://doi.org/10.1016/j.ijbiomac.2017.03.167.

Niu, F., Hu, D., Gu, F., Du, Y., Zhang, B., Ma, S., Pan, W., 2021. Preparation of ultra-long stable ovalbumin/sodium carboxymethylcellulose nanoparticle and loading properties of curcumin. Carbohydr. Polym. 271, 118451 https://doi.org/10.1016/j.carbpol.2021.118451.

Patel, A.R., Bouwens, E.C.M., Velikov, K.P., 2010. Sodium caseinate stabilized zein colloidal particles. J. Agric. Food Chem. 58 (23), 12497–12503. https://doi.org/10.1021/jf102959b.

Patle, T.K., Shrivas, K., Kurrey, R., Upadhyay, S., Jangde, R., Chauhan, R., 2020. Phytochemical screening and determination of phenolics and flavonoids in Dillenia pentagyna using UV–vis and FTIR spectroscopy. Spectrochim. Acta 242, 118717. https://doi.org/10.1016/j.saa.2020.118717.

Peinado, I., Lesmes, U., Andres, A., McClements, D.J., 2010. Fabrication and morphological characterization of biopolymer particles formed by electrostatic complexation of heat treated lactoferrin and anionic polysaccharides. Langmuir 26 (12), 9827–9834. https://doi.org/10.1021/la1001013.

Porter, C.J.H., Trevaskis, N.L., Charman, W.N., 2007. Lipids and lipid-based formulations: optimizing the oral delivery of lipophilic drugs. Nat. Rev. Drug Discov. 6 (3), 231–248. https://doi.org/10.1038/nrd2197.

Rampino, A., Borgogna, M., Bellich, B., Blasi, P., Virgilio, F., Cesàro, A., 2016. Chitosan-pectin hybrid nanoparticles prepared by coating and blending techniques. Eur. J. Pharmaceut. Sci. 84, 37–45. https://doi.org/10.1016/j.ejps.2016.01.004.

Siemińska-Kuczer, A., Szymańska-Chargot, M., Zdunek, A., 2022. Recent advances in interactions between polyphenols and plant cell wall polysaccharides as studied using an adsorption technique. Food Chem. 373, 131487 https://doi.org/10.1016/j.foodchem.2021.131487.

Sun, C., Liu, F., Yang, J., Yang, W., Yuan, F., Gao, Y., 2015. Physical, structural, thermal and morphological characteristics of zein quercetagetin composite colloidal nanoparticles. Ind. Crop. Prod. 77, 476–483. https://doi.org/10.1016/j.indcrop.2015.09.028.

Sun, C.X., Dai, L., Gao, Y.X., 2017. Formation and characterization of the binary complex between zein and propylene glycol alginate at neutral pH. Food Hydrocolloids 64, 36–47. https://doi.org/10.1016/j.foodhyd.2016.10.031.

Teixe-Roig, J., Oms-Oliu, G., Balleste-Munoz, S., Odriozola-Serrano, I., Martin-Belloso, O., 2020. Improving the in vitro bioaccessibility of beta-carotene using pectin added nanoemulsions. Foods 9 (4). https://doi.org/10.3390/foods9040447.

Tomas, M., Rocchetti, G., Ghisoni, S., Giuberti, G., Capanoglu, E., Lucini, L., 2020. Effect of different soluble dietary fibres on the phenolic profile of blackberry puree subjected to in vitro gastrointestinal digestion and large intestine fermentation. Food Res. Int. 130, 108954 https://doi.org/10.1016/j.foodres.2019.108954.

Torres, O., Tena, N.M., Murray, B., Sarkar, A., 2017. Novel starch based emulsion gels and emulsion microgel particles: design, structure and rheology. Carbohydr. Polym. 178, 86–94. https://doi.org/10.1016/j.carbpol.2017.09.027.

Wang, G., Yu, B., Wu, Y., Huang, B., Yuan, Y., Liu, C.S., 2013. Controlled preparation and antitumor efficacy of vitamin E TPGS-functionalized PLGA nanoparticles for delivery

of paclitaxel. Int. J. Pharm. 446 (1–2), 24–33. https://doi.org/10.1016/j.ijpharm.2013.02.004.

Wang, X., Peng, F., Liu, F., Xiao, Y., Li, F., Lei, H., Wang, J., Li, M., Xu, H., 2020. Zein-pectin composite nanoparticles as an efficient hyperoside delivery system: fabrication, characterization, and in vitro release property. LWT 133, 109869. https://doi.org/10.1016/j.lwt.2020.109869.

Willats, W.G.T., Knox, J.P., Mikkelsen, J.D., 2006. Pectin: new insights into an old polymer are starting to gel, Trends. Food Sci. Technol. 17 (3), 97–104. https://doi.org/10.1016/j.tifs.2005.10.008.

Xu, G., Li, L., Bao, X., Yao, P., 2020. Curcumin, casein and soy polysaccharide ternary complex nanoparticles for enhanced dispersibility, stability and oral bioavailability of curcumin. Food Biosci. 35, 100569 https://doi.org/10.1016/j.fbio.2020.100569.

Yan, J.K., Qiu, W.Y., Wang, Y.Y., Wu, J.Y., 2017. Biocompatible polyelectrolyte complex nanoparticles from lactoferrin and pectin as potential vehicles for antioxidative curcumin. J. Agric. Food Chem. 65 (28), 5720–5730. https://doi.org/10.1021/acs.jafc.7b01848.

Ying, X., Lu, X., Sun, X., Li, X., Li, F., 2007. Determination of vitexin-2''-O-rhamnoside in rat plasma by ultra-performance liquid chromatography electrospray ionization tandem mass spectrometry and its application to pharmacokinetic study. Talanta 72 (4), 1500–1506. https://doi.org/10.1016/j.talanta.2007.01.059.

Zhao, X., Zhang, X., Tie, S., Hou, S., Wang, H., Song, Y., Rai, R., Tan, M., 2020. Facile synthesis of nano-nanocarriers from chitosan and pectin with improved stability and biocompatibility for anthocyanins delivery: an in vitro and in vivo study. Food Hydrocolloids 109. https://doi.org/10.1016/j.foodhyd.2020.106114.

Zhou, J.F., Zheng, G.D., Wang, W.J., Yin, Z.P., Chen, J.G., Li, J.E., Zhang, Q.F., 2021. Physicochemical properties and bioavailability comparison of two quercetin loading zein nanoparticles with outer shell of caseinate and chitosan. Food Hydrocolloids 120, 106959. https://doi.org/10.1016/j.foodhyd.2021.106959.

Zhu, X.X., Li, L.D., Liu, J.X., Liu, Z.Y., Ma, X.Y., 2006. Effect of vitexia-rhamnoside (V-R) on vasomotor factors expression of endothelial cell. China J. Chin. Mater. Med. 31 (7), 566–569.

Zhu, K.K., Ye, T., Liu, J.J., Peng, Z., Xu, S.S., Lei, J.Q., Deng, H.B., Li, B., 2013. Nanogels fabricated by lysozyme and sodium carboxymethyl cellulose for 5-fluorouracil controlled release. Int. J. Pharm. 441 (1–2), 721–727. https://doi.org/10.1016/j.ijpharm.2012.10.022.